CHAPTER 3 PRELIMINARY TWO-DIMENSIONAL STUDY

3.1 INTRODUCTION

This chapter describes a two-dimensional analysis of pipe joint behaviour. More detailed three-dimensional analyses are described in later chapters. For the two-dimensional analysis described in this chapter, the finite element program OXFEM (Burd 1996) was used. The program contains simple elastic-plastic material models and various types of elements including interface elements used to simulate the interaction between the concrete pipe and the packing material. The mesh generation program OXMESH (Houlsby 1988) available in the Civil Engineering Research Group at the Department of Engineering Science was used to generate the finite element meshes.

The main purpose of this preliminary study is to provide experience with the use of interface elements for interaction between the pipe and the packing material, numerical material models and non-linear analysis procedure. In this chapter, a simplified two-dimensional numerical model is described in Section 3.2. The effect of the properties of the packing material and the effect of the misalignment of the pipeline are discussed in Sections 3.3 and 3.4 respectively. Finally, Section 3.5 gives the conclusion.

3.2 TWO-DIMENSIONAL MODEL

In the two-dimensional analysis, the pipe wall instead of the complete pipe was examined. Although the concrete pipe, loading condition and boundary conditions in pipe jacking are three-

dimensional in nature, a small region of the concrete pipe walls around the joint including the packing material was simplified as a plane strain model in order to carry out some simple, preliminary, calculations. The simplified numerical model and its finite element mesh are shown in Figure 3.1(a) and 3.1(b) respectively. The dimensions of the model are also given in the figure. In the analysis, the nodes at the bottom of the lower pipe (it is actually a small region of the pipe wall but is referred to as 'pipe' in this chapter for simplicity) were pinned, which leads to a pipe boundary condition that is effectively fixed. The strength of the jacking pipe is approximately 65MPa as discussed in Chapter One. The maximum pressure on the pipe end in practice should be less than 30MPa for safety reasons. In this simple model, a uniform pressure q = 30MPa was applied vertically to the top of the upper pipe to simulate the thrust force during pipe jacking and the upper pipe was rotated through a small angle β to simulate the misalignment of the pipeline. In the analysis, this misalignment angle β was simulated by an equivalent given displacement δ in the x direction at the top of the upper pipe. Equivalence here means that if the displacement in the x direction at the bottom of the upper pipe is zero, the displacement δ at the top would produce the same rotation angle β (that is, $\tan\beta = \delta / L$, $L = 150$mm is the length of the 'pipe'). The load and the misalignment rotation were applied simultaneously in the numerical analysis. To examine the influence of the misalignment angle, two different misalignment angles $\beta = 0.1^0$ and 0.3^0 were studied in the analysis (the equivalent displacements at the top of the upper pipe in x direction for $\beta = 0.1^0$ and 0.3^0 are 0.26mm and 0.79mm respectively).

In the numerical analysis, the concrete pipe and the packing material were assumed to be linearly elastic. The material constants of the concrete pipe were chosen with a typical shear modulus $G_c = 40000$MPa and a Poisson's ratio $\mu_c = 0.20$. The main type of element used in the

mesh was 6-node triangle. A layer of 6-node line interface elements was used on each interface between the pipe and the packing material to simulate the interaction between them. The stiffness of the interface should be high in theory. However, high interface stiffness could cause calculation difficulties in analysis. According to the research carried out by Burd (1986), Beer (1985), Burd and Brocklehurst (1992), and Adhikary and Dysin (1998), the stiffness of the interface was chosen in such a way that the deformation of the interface is about 5 percent of that of the packing material. With reference to the properties and dimensions of the packing material, the properties of the interface model were chosen with the normal stiffness Kn = 800MPa /mm, the shear stiffness Ks = 400MPa /mm, the frictional angle $\phi = 20^0$ and the dilation angle $\psi = 20^0$. To assess the sensitivity of the stiffness of the interface in this model, analyses were also carried out with high interface stiffness Kn = 8000MPa /mm and Ks = 4000MPa /mm. The modified Euler iteration procedure (Burd 1986) was used for this preliminary analysis and the total number of calculation steps was 400.

3.3 EFFECT OF PACKING MATERIAL PROPERTIES

The experimental research by Milligan and Ripley (1989), Ripley (1989), Husein (1989), and Boot and Husein (1991) has shown that packing materials play an important role in pipe jacking by reducing the stress concentration at the pipe joint which in turn reduces the risk of pipe damage. In order to understand the interaction between the packing material and the pipe, a parametric study has been carried out to examine the influence of the properties of the packing materials using the two-dimensional model. The research carried out by Milligan and Ripley (1989) and Husein (1989) showed that the stiffness of the packing material could vary from about

260MPa for plywood and chipboard to 2600MPa for nylon, and that the Poisson's ratio would change from almost zero for plywood and chipboard to almost 0.5 for LDPE and Elastomer. In the analyses, three typical Poisson's ratios of the packing material, μ_p = 0.1, 0.4 and -0.3 representing low, high and negative Poisson's ratios with a typical shear modulus G_p = 300MPa were studied for the influence of the Poisson's ratio; and three typical shear moduli G_p = 300MPa, 600MPa and 900MPa with μ_p = 0.1 were included to examine the influence of the stiffness of the packing material (the stiffness of the packing material is $E_p = 2\,G_p(\,1 + 2\mu_p\,)$, and shear modulus and Poisson's ratio are the input data of the material constants in program OXFEM).

The normal stresses on the lower interface with $\beta = 0.1^0$ are shown in Figure 3.2. The figure shows that the normal stresses are approximately linearly distributed with x on the interface with their maximum magnitudes in the right end region (x=150mm) except in the case of $\mu_p = 0.4$ where the magnitude of normal stress is higher in the middle area on the interface and highly non-linear at the two end regions. In general, packing material with higher shear modulus induces higher maximum normal stress with the same Poisson's ratio. The influence of the Poisson's ratio of the packing material is complex, packing material with both high and negative Poisson's ratio induce higher non-linearity at the two end regions. However, the normal stress in the case of $\mu_p = -0.3$ is close to that in the case of $\mu_p = 0.1$, while the magnitude of the normal stress in the case of $\mu_p = 0.4$ is higher in the middle area on the interface.

The shear stresses on the lower interface with $\beta = 0.1^0$ are shown in Figure 3.3. The figure shows that in the case of $\mu_p = 0.1$ the distribution patterns are similar for different packing materials with different shear modulus, that is, the shear stresses are almost constant and small on

the interface except in the two end regions, and that packing material with higher shear modulus induces slightly higher shear stress on the interface. In the cases of $\mu_p = 0.4$ and $\mu_p = -0.3$, the shear stresses are also small in the middle area, however, the magnitude of the shear stresses are high in the two end regions. The direction of the shear stresses at the two end regions is towards the centre in the case of $\mu_p = -0.3$ and in the opposite direction in the other case. (The stresses on the interface are calculated at Gauss points and the shear stresses at each end ($x = 0$mm and 150mm) of the interface are zero because there is no shear stress on the plane $x = 0$ and $x = 150$mm .)

The most tensile principal stresses around the joint with $\beta = 0.1^0$ are shown in Figure 3.4(a), 3.4(b), 3.4(c) and 3.4(d) for the case of $\mu_p = 0.1$, $\mu_p = 0.4$ and $\mu_p = -0.3$ with $G_p = 300$MPa, and $\mu_p = 0.1$ with $G_p = 900$MPa respectively. From the figure, it is clear that the tensile stresses are mainly located in the region of the pipe joint while the tensile stresses are very small in other regions. Moreover, the results indicate that with the same shear modulus $G_p = 300$MPa, packing materials with a high Poisson's ratio ($\mu_p = 0.4$) generate much larger tensile stresses in the concrete than those with a lower Poisson's ratio ($\mu_p = 0.1$) due to the high shear stresses on the interface in the case of $\mu_p = 0.4$ as shown in Figure 3.3, and that if a negative Poisson's ratio is used for the packing material then tensile stresses in the concrete are almost zero (high tensile stresses appear in the packing material). With the same Poisson's ratio ($\mu_p = 0.1$), packing material with higher shear modulus $G_p = 900$MPa also produce higher tensile stresses in the concrete, although the influence is not significant compared with that of the Poisson's ratio.

In order to assess the sensitivity of the stiffness of the interface, analyses were also carried out with high interface stiffness Kn = 8000MPa /mm and Ks = 4000MPa /mm while other conditions were unchanged. Figure 3.5 shows the most tensile principal stresses around the joint with $\beta = 0.1^0$ and the high interface stiffness. Comparing with the stresses in Figure 3.4, it is clear that both the stress distribution patterns and the maximum stresses are similar. This means that the influence of the interface stiffness on the computed stresses is small in this model. This is why the same material constants of the interface were used in this chapter for all the analyses with different packing materials.

3.4 EFFECT OF THE PIPELINE MISALIGNMENT

This section describes the parametric study with a high misalignment angles $\beta = 0.3^0$ to examine the influence of the amount of the pipeline misalignment. The analyses were carried out with the properties of the packing material and other conditions unchanged as in Section 3.3. The normal stresses on the lower interface with $\beta = 0.3^0$ are shown in Figure 3.6. Again, the normal stresses are approximately linearly distributed with x on the interface with their maximum magnitude at the right end region (x = 150mm). In general, the normal stresses are more localized than those with $\beta = 0.1^0$. Again, with the same Poisson's ratio, packing material with higher shear modulus induces higher maximum normal stress on the interface. With the same shear modulus (G_p = 300MPa), the normal stresses in the case of $\mu_p = 0.1$ and -0.3 are somewhat similar, while the normal stresses in the case of $\mu_p = 0.4$ are more localized. This means that the influence of the packing material on the normal stresses on the interface is not only due to the change of the

stiffness of the packing material $E_p = 2\ G_p (1 + 2\ \mu_p)$ but also due to the change of the Poisson's ratio of the packing material.

The shear stresses on the lower interface with $\beta = 0.3^0$ are shown in Figure 3.7. The distribution patterns of the shear stress on the interface are similar to those with $\beta = 0.1^0$ in Section 3.3 but the magnitudes of the shear stresses are higher. The influence of the properties of the packing material are also similar to that in the case with $\beta = 0.1^0$ (refer to Section 3.3, see Figure 3.3).

The most tensile principal stresses around the joint with $\beta = 0.3^0$ are shown in Figure 3.8(a), 3.8(b), 3.8(c) and 3.8(d) for the case of $\mu_p = 0.1$, $\mu_p = 0.4$ and $\mu_p = -0.3$ with $G_p = 300$MPa, and $\mu_p = 0.1$ with $G_p = 900$MPa respectively. Again, the tensile stresses are mainly located in the region of the pipe joint. The stress distribution patterns and the influence of the properties of the packing material are similar to those with $\beta = 0.1^0$ as shown in Figure 3.4, however, the maximum tensile stress is much higher. (The scale in Figure 3.4 is different from that in Figure 3.8.)

3.5 CONCLUSION

The results in this chapter show that the pipeline misalignment causes high shear stresses and localization of the normal stresses on the interface which in turn may generate high tensile stresses and concentrations of compressive stress in the concrete. Moreover, the effect of the misalignment

is coupled with the effect of the Poisson's ratio and the shear modulus of the packing material. That is, the higher the value of β, the higher the peak value of the stresses with the same μ_p and G_p, and the higher the value of μ_p and/or G_p, the higher the peak value of stresses with the same β.

From the numerical results of the simplified two-dimensional model in this chapter, a few conclusions may be drawn:

(1) The packing material with high Poisson's ratio ($\mu_p = 0.4$) induces higher tensile stresses at the pipe joint than that with low Poisson's ratio ($\mu_p = 0.1$). The packing material with negative Poisson's ratio produces even better results although the result difference is not significant between the low Poisson's ratio and the negative Poisson's ratio.

(2) Material with high shear stiffness increases the stresses on the interface and in the pipe, although the influence of the shear stiffness on the stresses is not significant compared with that of the Poisson's ratio.

(3) Misalignment of the pipeline is the main factor for inducing both high tensile stresses and high compressive stresses at the pipe joint. The higher the misalignment angle, the higher the tensile stresses in the concrete pipe.

(4) Interface elements are useful for the study of contact problems because they can simulate the interaction between different structures and be used to extract details about the stress distribution on the interface. The influence of the stiffness of the interface on the computed stresses is small in this model.

(5) The main purpose of the two-dimensional model is to gain experience. The results need to be verified with three-dimensional models due to the three-dimensional nature of the problem.

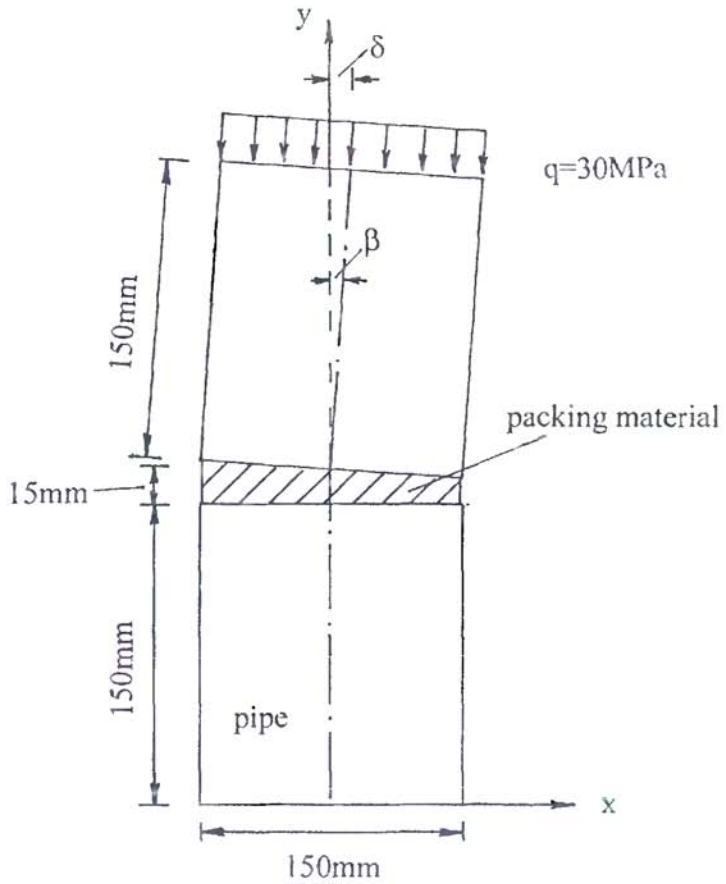

(a) Two-dimensional model

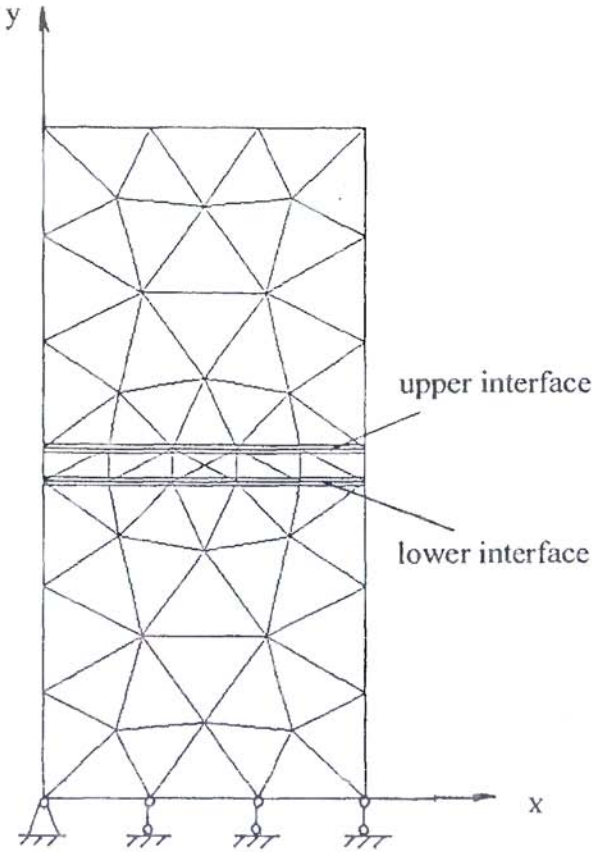

(b) Finite element mesh

Figure 3.1 Simplified model and its finite element mesh

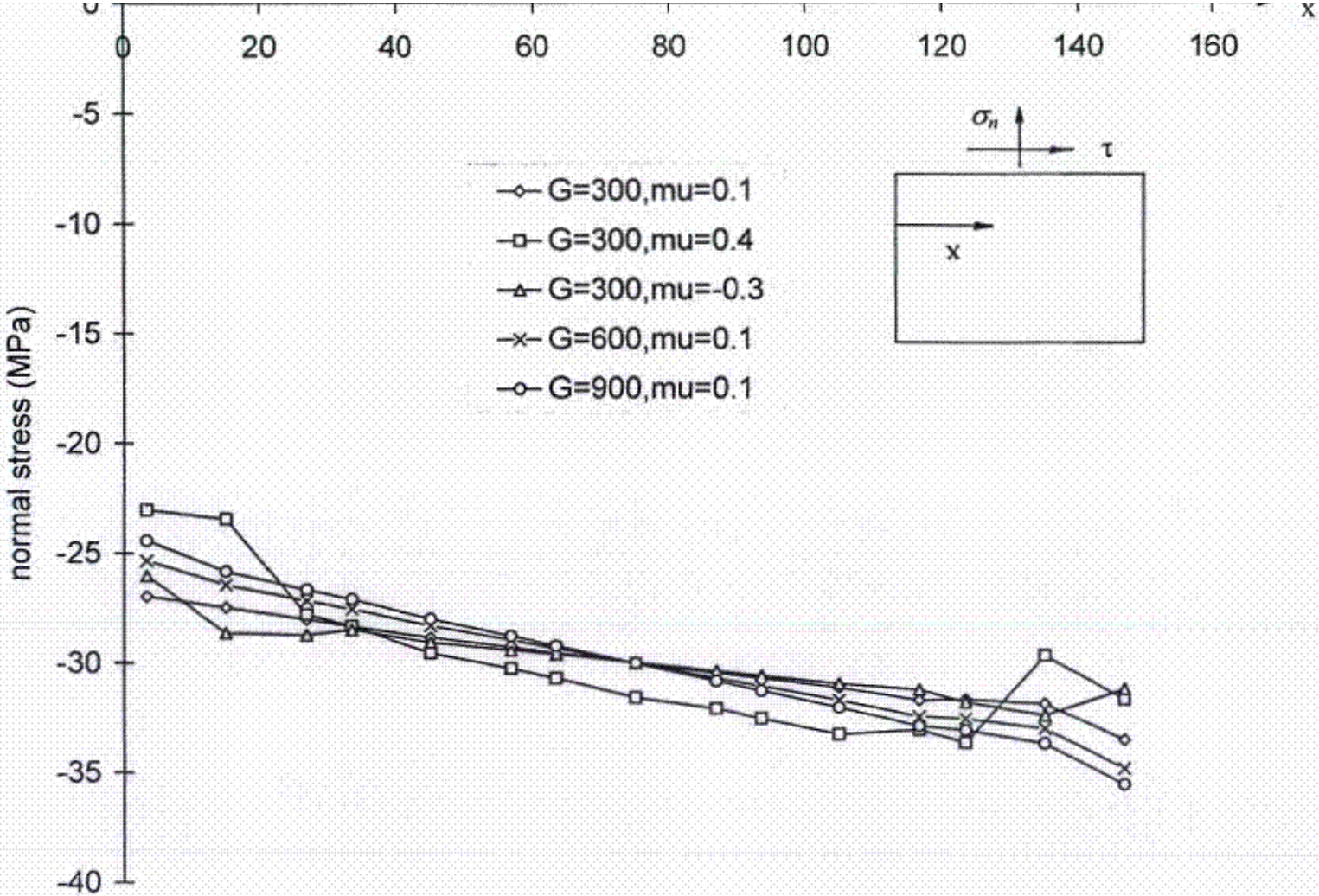

Figure 3.2 Normal stresses on the lower interface with $\beta=0.1^0$

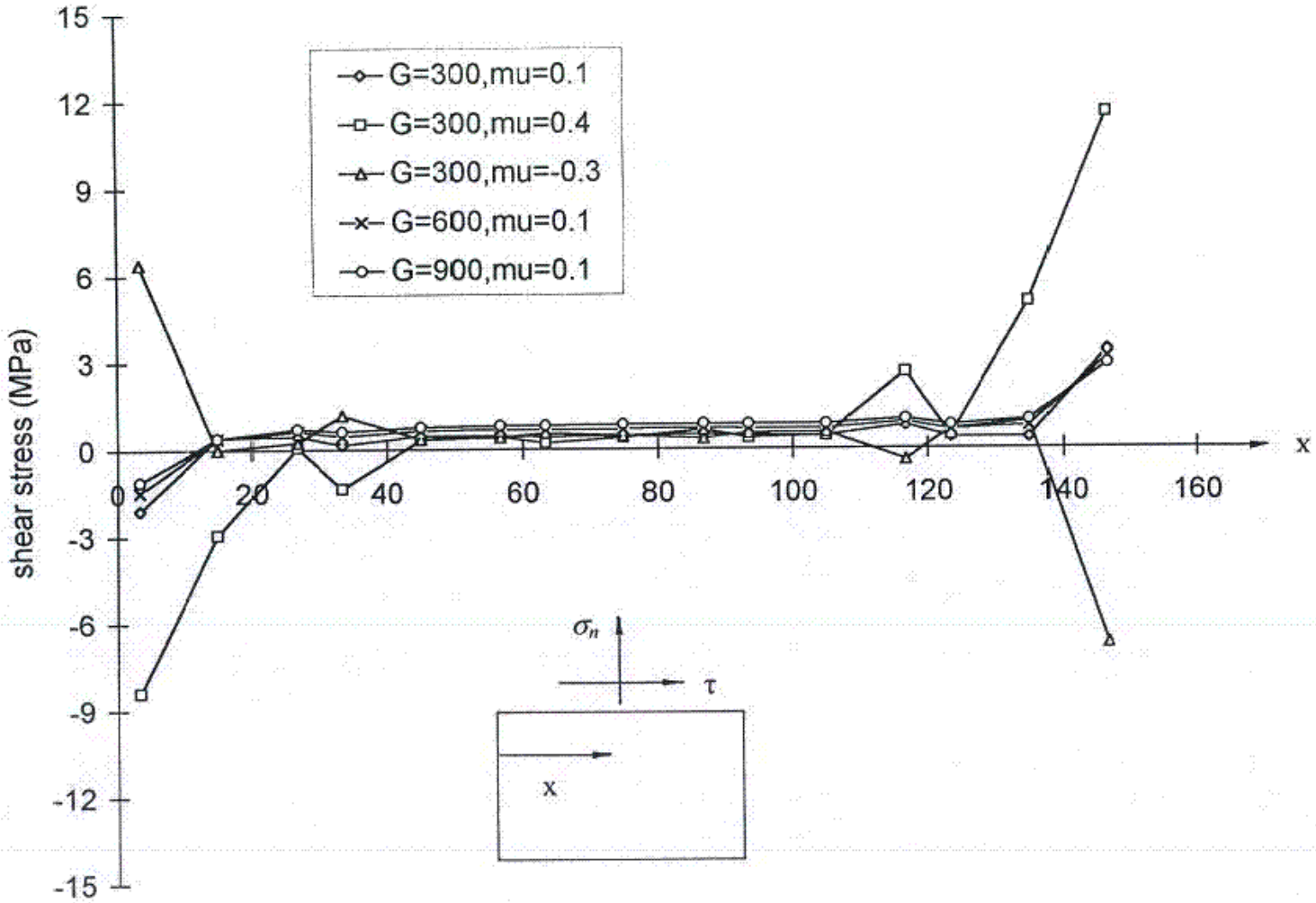

Figure 3.3 Shear stresses on the lower interface with $\beta=0.1^0$

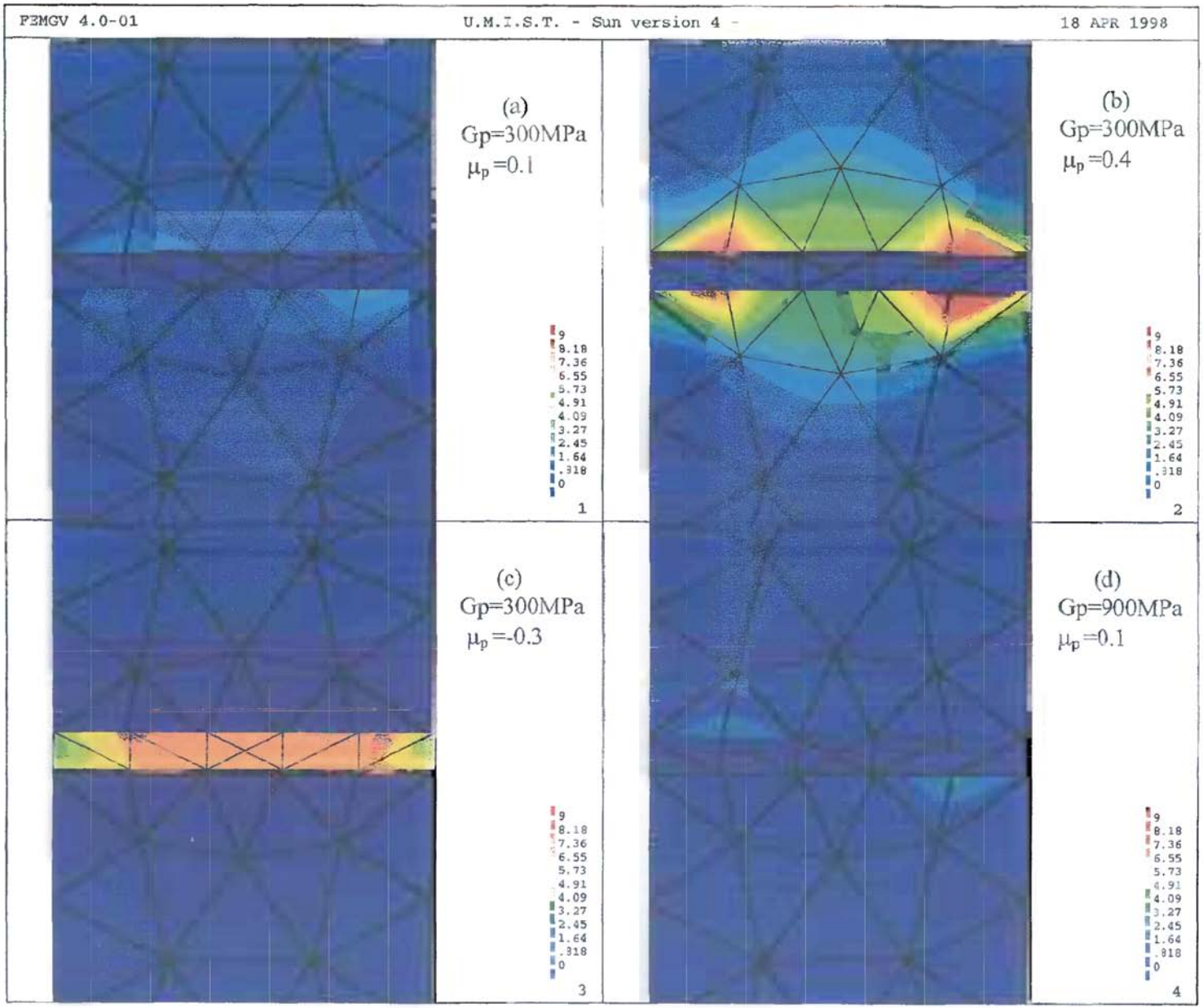

Figure 3.4 Most tensile principal stresses at the joint with $\beta=0.1^0$ (MPa)

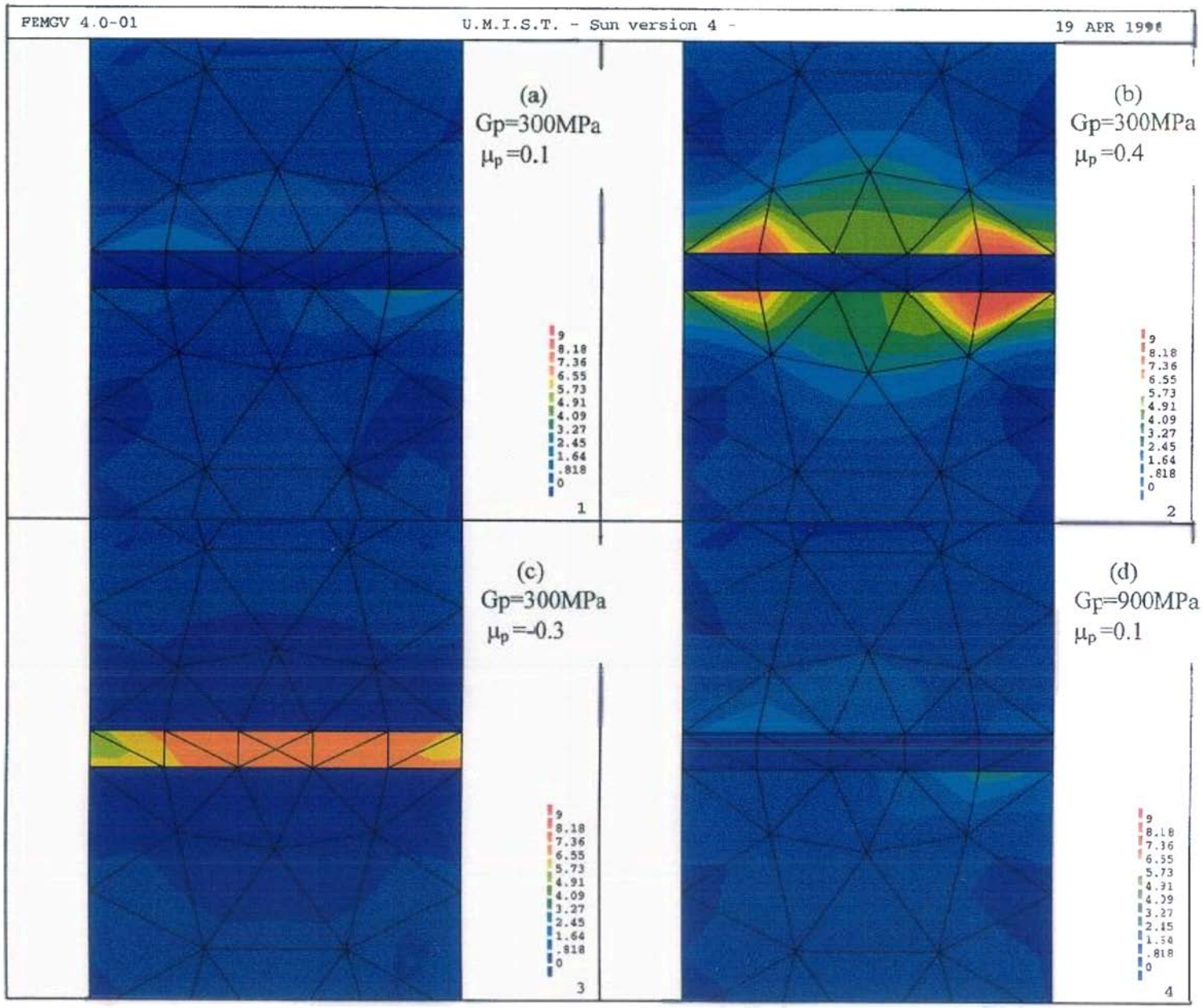

Figure 3.5 Most tensile principal stresses at the joint with $\beta=0.1^0$ and high interface stiffness (MPa)

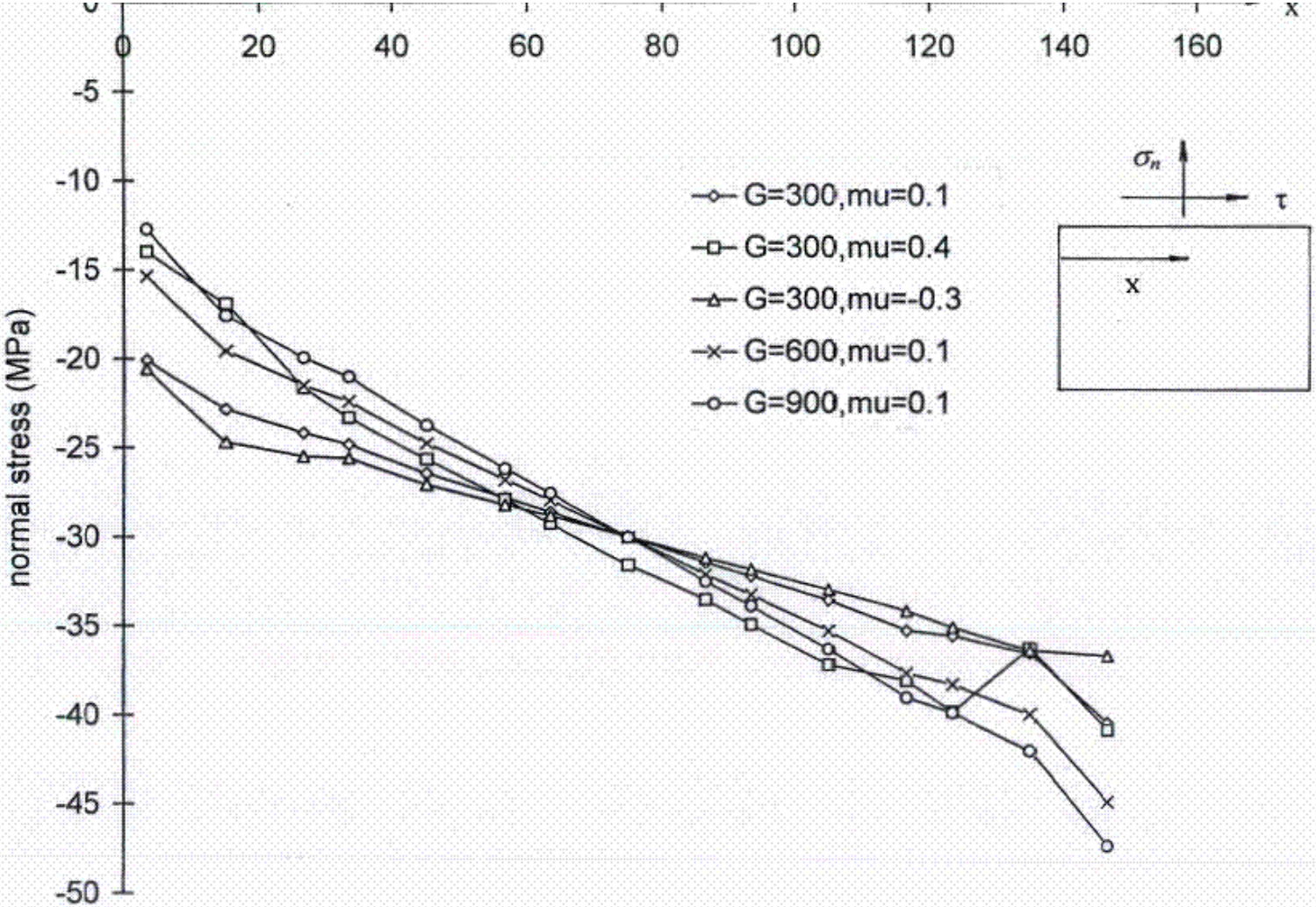

Figure 3.6 Normal stresses on the lower interface with $\beta=0.3^0$

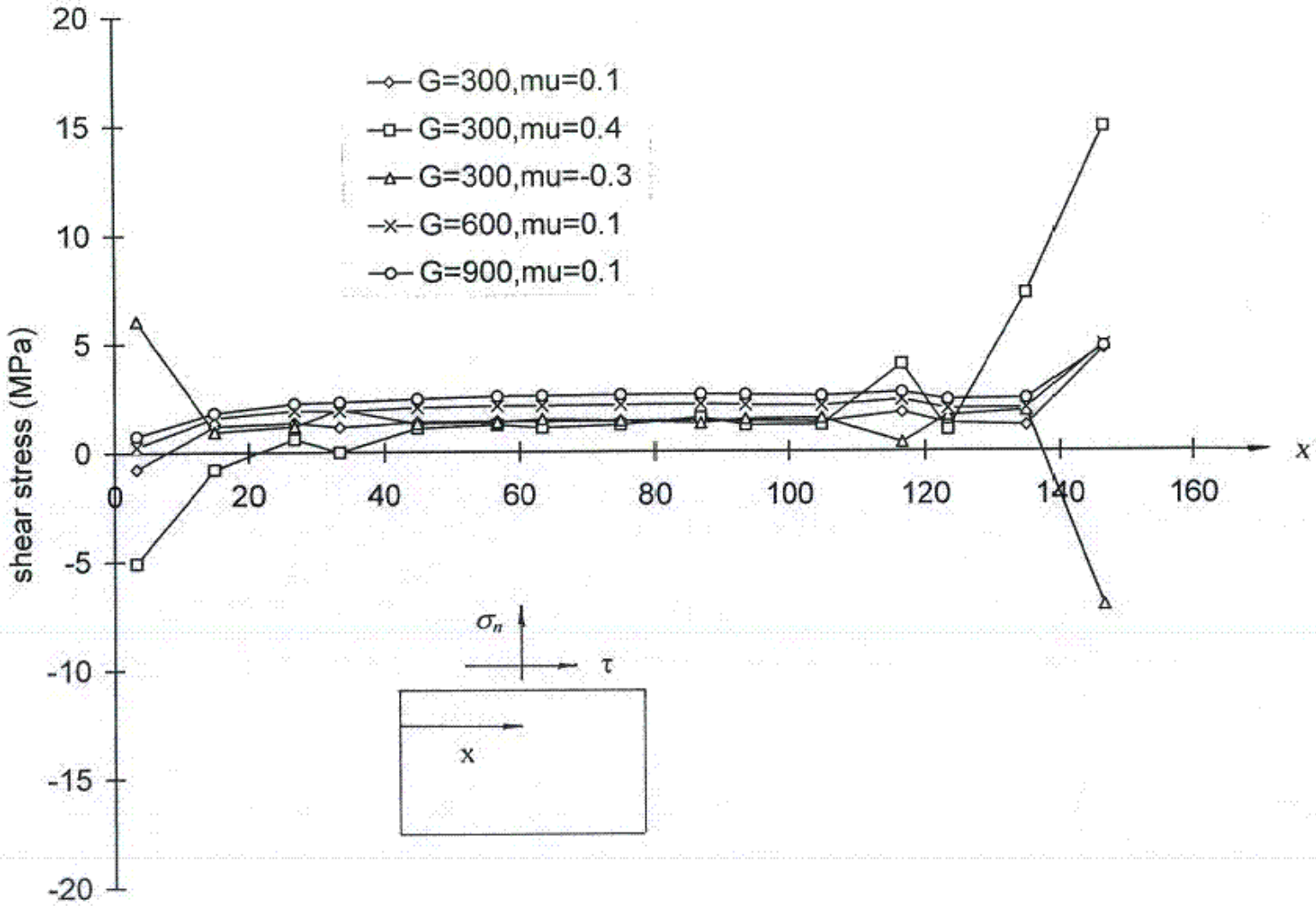

Figure 3.7 Shear stresses on the lower interface with $\beta=0.3^0$

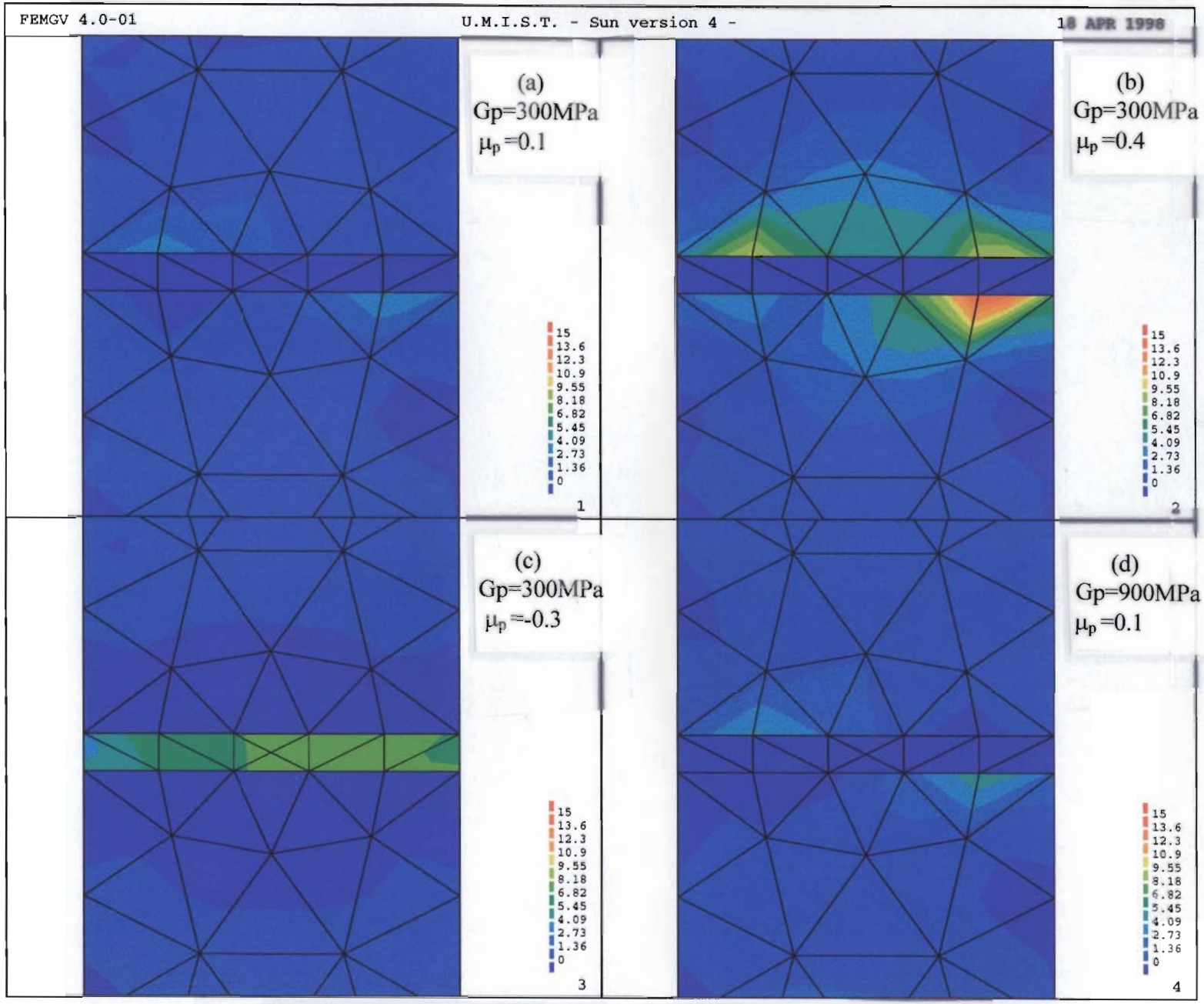

Figure 3.8 Most tensile principal stresses at the joint with $\beta=0.3^0$ (MPa)